British Journal of Pharmaceutical Research
3(3): 326-346, 2013

SCIENCEDOMAIN *international*
www.sciencedomain.org

Design and Characterization of Glyceryl Monostearate Solid Lipid Nanoparticles Prepared by High Shear Homogenization

A. R. Gardouh[1], Shadeed Gad[1], Hassan M. Ghonaim[1,2*] and Mamdouh M. Ghorab[1]

[1]Department of Pharmaceutics and Industrial Pharmacy, Faculty of Pharmacy, Suez Canal University, Ismailia 41522, Egypt.
[2]Institute of Life Sciences Research, University of Bradford, Bradford, BD7 1RD, UK.

Authors' contributions

This work was carried out in collaboration between all authors. Author ARG designed the study, wrote the protocol, and wrote the first draft of the manuscript. Author HMG managed the analyses of the study, managed the literature searches and overall revision and submission. Authors SG, HMG and MMG supervised the entire research. All authors read and approved the final manuscript.

Research Article

Received 12th December 2012
Accepted 19th February 2013
Published 19th March 2013

ABSTRACT

Aims: The aim of this study was to explore the practicability of preparation of solid lipid nanoparticles of Glyceryl monostearate containing Dibenzoyl peroxide, Erythromycin base, and Triamcinolone acetonide as model drugs. The physicochemical properties of the prepared formulae like particle size, drug entrapment efficiency, drug loading capacity, yield content and in-vitro drug release behavior were also measured.
Methodology: Solid lipid nanoparticles loaded with three model lipophilic drugs were prepared by high shear hot homogenization method. The model drugs used are Dibenzoyl peroxide, Erythromycin base, and Triamcinolone acetonide. Glyceryl monostearate was used as lipid core; Tween 20 and Tween 80 were employed as surfactants and lecithin as co-surfactant. Many formulation parameters were controlled to obtain high quality nanoparticles. The prepared solid lipid nanoparticles were evaluated by different standard physical and imaging methods. The efficiency of drug release form prepared formulae was studied using *in vitro* technique with utilize of dialysis bag technique. The stability of

**Corresponding author: Email: hassan_ghonaim@pharm.suez.edu.eg;*

prepared formulae was studied by thermal procedures and infrared spectroscopy.
Results: The mean particle diameter measured by laser diffraction technique was (194.6±5.03 to 406.6±15.2 nm) for Dibenzoyl peroxide loaded solid lipid nanoparticles, (220±6.2 to 328.34±2.5) nm for Erythromycin loaded solid lipid nanoparticles and (227.3±2.5 to 480.6±24) nm for Triamcinolone acetonide loaded solid lipid nanoparticles. The entrapment efficiency and drug loading capacity, determined with ultraviolet spectroscopy, were 80.5±9.45% and 0.805±0.093%, for Dibenzoyl peroxide, 96±11.5 and 0.96±0.012 for Triamcinolone acetonide and 94.6±14.9 and 0.946±0.012 for Erythromycin base respectively. It was found that model drugs showed significant faster release patterns when compared with commercially available formulations and pure drugs ($p<0.05$). Thermal analysis of prepared solid lipid nanoparticles gave indication of solubilization of drugs within lipid matrix. Fourier Transformation Infrared Spectroscopy (FTIR) showed the absence of new bands for loaded solid lipid nanoparticles indicating no interaction between drugs and lipid matrix and being only dissolved in it. Electron microscope of scanning and transmission techniques indicated sphere form of prepared solid lipid nanoparticles with smooth surface with size below 100 nm.
Conclusions: Solid lipid nanoparticles with small particle size have high encapsulation efficiency, and relatively high loading capacity for Dibenzoyl peroxide, Erythromycin base, and Triamcinolone acetonide as model drugs can be obtained by this method.

Keywords: Solid lipid nanoparticles; high shear homogenization; tween 20; tween 80; glyceryl monostearate; dibenzoyl peroxide; erythromycin base; triamcinolone acetonide.

1. INTRODUCTION

Solid lipid nanoparticles (SLN) offer an attractive means of drug delivery, particularly for poorly water-soluble drugs. They combine the advantages of polymeric nanoparticles [1] fat emulsions and Liposomes [2,3]. SLN consist of drug trapped in biocompatible lipid core and surfactant at the outer shell, offering a good alternative to polymeric systems [4] in terms of lower toxicity [5]. Moreover, the production process can be modulated for desired drug release, protection of drug degradation and avoidance of organic solvents. The previous advantages make SLN a promising carrier system for optimum drug delivery. Dibenzoyl peroxide is a safe and effective agent for treating acne. Dibenzoyl peroxide has no direct effect on inflammation and works through its bactericidal actions [6]. Furthermore, Dibenzoyl peroxide's lipophilic nature enhances transport through sebaceous glands, with maximum penetration through acne follicles. Dibenzoyl peroxide can be attached to the solid lipid nanoparticles surface and facilitate drug targeting to skin strata and increase efficiency of acne remedy [7].

Topical erythromycin treatment was used for inflammatory acne vulgaris due to activity against *Propionibacterium acnes* [8]. It is slightly soluble in water, freely soluble in alcohol, soluble in methanol.

Triamcinolone acetonide is a topical lipophilic corticosteroid used to treat dermatitis [9].Dibenzoyl peroxide, erythromycin base and triamcinolone acetonide are examples of topical drugs with poor dermal localization due to lipophilicity. Solid lipid nanoparticles could be a carrier for these drugs with potential impact on dissolution of these drugs.
The aim of this study was to explore the practicability of preparation of solid lipid nanoparticles containing Dibenzoyl peroxide (DP), Erythromycin base(ER), and

Triamcinolone acetonide (TA). High shear hot homogenization technique was employed to prepare the solid lipid nanoparticles; the physicochemical properties of the SLNs like particle size, drug entrapment efficiency (EE), drug loading capacity(LC), yield content and in-vitro drug release behavior were studied.

2. METHODOLOGY

2.1 Materials

Glyceryl monostearate-technical self-emulsifying (BDH Chemicals Ltd Poole-England), Tween 80 (polysorbate 80), Tween 20 (polysorbate 20), ICI America (Wilmington, DE, USA), Lecithin (Spectrum Chemicals & Laboratory Products, New Brunswick, NJ), Dibenzoyl peroxide, triamcinolone acetonide, erythromycin base (MUP pharmaceutical company, Abu sultan, Egypt), Aknemycin® cream, Akenroxide® gel (MUP pharmaceutical company, Abusultan, Egypt), Kenalog® cream (Bristol–Myers squib), Dialysis tubing cellulose membrane (molecular weight cut-off 12,000 g/mole) sigma-Aldrich Chemical Company, St.Louis, USA, and all other chemicals were of reagent grade and used as delivered.

2.2 Methods

2.2.1 Preparation of solid lipid nanoparticles loaded with model drugs

Solid lipid nanoparticles of the smallest size during preliminary study were loaded with DP, ER and TA as model topical drugs. Briefly, the drugs were dispersed in melted lipid (60-70^0), then the mixture was dispersed in a hot aqueous solution with surfactant concentration of 5 % w/w and 1 % w/w lecithin as co-surfactant at the same temperature, by high –speed stirring, using an Ultra-Turrax homogenizer (Ultra- Turrax T – 25, IKA, Germany) at 12, 000 rpm for 10 minutes, with 30 seconds intervals every two minutes. The resulting dispersion was then cooled and each sample was diluted with water before measurement and particle size was measured using dynamic laser light scattering apparatus at 25 ºC. (Mastersizer 2000 vers. 5.54, hydro 2000 S, Malvern instruments Ltd., Malvern, Worcs, UK). Each measurement was performed in triplicate and the particle average diameter and polydispersity index (PI) were determined [10]. SLNs were prepared by the same technique using 50 % w/w glycerol as viscosity enhancer.

2.2.2 Loading capacity

The loading capacity (L.C) refers to the percentage amount of drug entrapped in solid lipid nanoparticles according to the following equation:

$$L.C. = \frac{\text{Total amount of drug} - \text{amount of unbound drug}}{\text{Nanoparticles weight}} X\ 100$$

2.2.3 Encapsulation efficiency

Drug entrapment efficiency was determined by ultracentrifugation. The drug entrapment efficiency was calculated from the ratio of the drug amount incorporated into SLNs to the total added drug amount. Ultracentrifugation was carried out using ultracentrifuge (Eppendorf centrifuge 5417 C, Netheler- Hinz- Gmbh), About 1 gm of SLNs dispersion

containing the drug was placed in the centrifuge tube, and samples were centrifuged at 14,000 rpm for 15 min. The amount of the drug in the supernatant was estimated spectrophotmetrically at 235 nm for DP according to B.P 2009[11], 250nm for TA according to B.P 2009[11] and 633 nm against a blank after ion pair with crystal violet for ER[12].

$$E.E. = \frac{\text{Total amount of drug – amount of unbound drug}}{\text{Total amount of drug}} \times 100$$

2.2.4 Determination of yield of solid lipid nanoparticles

This was calculated by weighing centrifuged samples of isolated solid lipid nanoparticles and referring them to the initial amount of solid lipid nanoparticles components according to the following equation

$$\text{Yield percentage (Y.P)} = \frac{\text{SLNs weight}}{\text{Total initial solids weight}} \times 100$$

Table 1. Composition of selected formulas used for loading of model drugs

Formula code	GMS %w/w	Surfactant % w/w	Co-surfactant % w/w (lecithin)	Glycerol %w/w
F1	10.0	5.0 (Tween 80)	1.0	----------
F2	10.0	5.0 (Tween 80)	1.0	50.0
F3	10.0	5.0 (Tween 20)	1.0	----------
F4	10.0	5.0 (Tween 20)	1.0	50.0

2.2.5 Scanning electron microscopy (SEM)

For scanning electron microscopy (SEM), dried solid lipid nanoparticles loaded with model drugs were fixed on a brass stub using double-sided adhesive tape and then made electrically conductive by coating with a thin layer of gold for 30 seconds using JEOL fine coat (JFC-1100F ion sputtering device) and scanned using JEOL (JSM-S.M 5300) using software (ORION 6.60.4).

2.2.6 Transmission electron microscopy (TEM)

Solid lipid nanoparticles loaded with model drugs were stained with phosphotungstic acid 2% w/v and placed on copper grids with Formvar films for viewing by a transmission electron microscope operated at 120 kV (JEOL-JEM-100CX EM) and operated using computer program named (AMT Image Capture Engine V601)

2.2.7 Differential scanning calorimetry (DSC)

Accurately weighed samples (1-8) mg samples were crimped in closed 40-µl aluminium pans. Samples were run at a heating rate of 10ºC /min under constant purging of nitrogen at 30ml/min and heated from 25 ºC to 300 ºC (except for samples of GMS ,it was heated to only 80 ºC and samples of DP to only 200 ºC) using Shimadzu DSC-60, Kyoto, Japan and Shimadzu DSC-60 data analysis. The references used for comparison were the same but empty aluminum pans.

2.2.8 Fourier transformation infrared spectroscopy (FTIR)

The pure drug, plain dried solid lipid nanoparticles, physical mixture and model drug loaded dried solid lipid nanoparticles were mixed for each with KBr (IR grade) in the ratio of 100: 1 and then scanned over a wave number range 4000- 500 cm^{-1}. Measurements were carried out using Shimadzu 435 U-O4 IR spectrometer, (Japan) at the Micro-Analytical Center of Faculty of Science, Cairo University, Egypt).

2.2.9 In- vitro drug release studies

These studies were completed using horizontal water bath shaker (Clifton water bath, USA) that maintained at 60 cycles per minute and the dialysis bag that could retain SLNs and allow the diffusion of free drug into dissolution media. The bags were soaked in distilled water for 12 h before use. The release medium was 10 ml phosphate buffer (pH 5.5). The temperature was set at 32 ± 0.5 ºC. A 1gm sample of the drug loaded SLNs was instilled in a dialysis bag held with two clamps at each end. At known time intervals (0.5, 1, 2, 4, 8, 12, 24, 36, and 48 h) the complete media were withdrawn and replaced by equal volumes of fresh buffer to maintain sink condition. The samples filtered and assayed for each model drug spectrophotometrically (Dibenzoyl peroxide at 235 nm, erythromycin base at 633 nm according to Amin and Issa [12] while triamcinolone acetonide at 250 nm with Shimadzu double beam UV- visible spectrophotometer model UV- 1601PC connected to a promax computer fitted with UPVC personal spectroscopy software version 3.7 (Shimadzu Corporation, Kyoto, Japan). The experiments were carried out as triplicate for each release study and the mean values were calculated [13].

Statistical analysis:

- All data were expressed as mean± SD.
- Data were analyzed by using the program SPSS 16.0 (SPSS Inc., Chicago, IL, USA) with help of one-way analysis of variance (ANOVA) test followed by post hoc multiple comparisons and(LSD) least significant difference formulae be significant at $P<0.05$.

3. RESULTS AND DISCUSSION

3.1 Particle Size of Prepared Solid Lipid Nanoparticles

Solid lipid nanoparticles of selected formulations listed in table (1) were loaded with model drugs were prepared using high shear hot homogenization with 12,000 rpm as homogenization speed.

Table (2) showed that the mean particle size measured by laser diffraction technique was 194.6±5.03 to 406.6±15.2 nm for Dibenzoyl peroxide loaded solid lipid nanoparticles, 220±6.2 to 328.34±2.5 for Erythromycin loaded solid lipid nanoparticles and 227.3±2.5 to 480.6±24 for Triamcinolone acetonide loaded solid lipid nanoparticles; while for empty solid lipid nanoparticles, particle size was from 172±3 nm to 231±11 nm. It was found that loading did not affect size of solid lipid nanoparticles. This result was in agreement with vivek et al [14] who found that lipid hydrophilicity, self-emulsifying properties of the lipid affected the shape of the lipid crystals (and hence the surface area) that had indirect effect on final size of the SLN dispersions. These results agreed with Le Verger et al [15] who compared empty

nanoparticles with that loaded with isradipine and found no significant difference between empty and loaded nanoparticles; solubility or dispersion of model drugs into nanoparticles beside high concentration of surfactant and co-surfactant may be a good reason for that. These results agreed with that of Almeida et al. [16] who stated that solid lipid nanoparticles are appropriate to incorporate lipophilic drugs that are dissolved in melted lipid.

3.2 Encapsulation Efficiency, Loading Capacity and Yield Content

Table (3) showed high relative encapsulation efficiency and drug loading. This may be due to high lipid concentration that enhances solubility of drugs and so loading of them into SLNs. These results agreed with that of Bhalekar et al [17]. The encapsulation efficiency in most formulations > 75% which may be due to higher ratio of lipid to drug (5:1). These results agreed with Kim et al [18] who found that loading of verapamil drug was > 75 % for all formulations having high lipid to verapamil ratio (5:1 and 10:1). The results showed high encapsulation efficiency and drug loading for formulations F1and F3 relative to F2 and F4; that may be attributed to the high viscosity of formulations F2 and F4. The presence of 50 % glycerol in previous formulae may hinder the loading of drugs into SLNs due to retardation of movement of particles. The encapsulation efficiency and drug loading of formulae F1 and F2 higher than F3 and F4, respectively due to use of Tween 80 with higher HLB than Tween 20 used for other formulae. Higher HLB values may enhance loading and encapsulation efficiency depending on reduction of interfacial tension and enhancement of solubilization of model drugs. These results were not in agreement with that of El-laithy et al [19] who prepared vinpocetine niosomes and found that the resulted product showed high encapsulation efficiency regardless of HLB of nonionic surfactants.

3.3 In-vitro Release Study

Membrane diffusion techniques are widely used for the study of drug in vitro release incorporated in colloidal systems. In these cases, drug release follows more than one mechanism. In case of release from the surface of SLNs, adsorbed drug quickly dissolved when it comes in contact with the release medium. Drug release by diffusion involves three steps. Briefly, water penetrates into system and causes swelling of matrix followed by the conversion of solid lipid into rubbery matrix, and then the diffusion of drug from the swollen rubbery matrix takes place. Hence, the release is slow initially and later, it becomes fast [20]. According to Le Verger et al. [15] the release rate of the drug and its appearance in the dissolution medium is controlled by partitioning the drug between the lipid phase and the aqueous environment in the dialysis bag then by diffusion of the drug across the membrane. The mode of preparation (cold or hot homogenization) influences the drug release profile. It was noted by Schafer –Korting et al [8] that surfactant and higher temperature enhanced prednisolone solubility in the aqueous phase and supported the enrichment of the steroid in the superficial layers during cooling of the preparation and crystallization of the lipid. Superficially entrapped prednisolone is available for the initial burst release.

Figures (1-3) showed that the release of drugs from formulae was enhanced significantly at level of $P<0.05$ when compared with drugs only, drugs mixed Tween 80 and drugs mixed with Tween 20 with the same proportions as in the formulae and also commercially available formulations.

Table 2. Particle Size and polydispersity index of empty SLNs and loaded SLNs

Formula code	Empty SLNs		DP-SLNs		ER-SLNs		TA-SLNs	
	Particle size(nm)± S.D	P.I	Particle size(nm)±S.D	P.I	Particle size (nm)± S.D	P.I	Particle size(nm)± S.D	P.I
F1	187±0.57	0.003	286±15.7	0.054	234±9.6	0.041	429±18	0.0419
F2	172±3	0.0104	194.6±5.03	0.0371	220±6.2	0.028	227.3±2.5	0.0109
F3	231±11	0.026	406.6±15.2	0.0376	273±10.5	0.008	480.6±24	0.0499
F4	180±1	0.007	356±13.5	0.0378	328.34±2.5	0.0109	352.67±7.6	0.030

Table 3. Yield percentage (Y.P), Encapsulation efficiency (E.E) and Loading capacity (L.C) of Loaded SLNs

Formula code	DP-SLNs			ER-SLNs			TA-SLNs		
	Y.P %	E.E %	L.C (ratio)	Y.P %	E.E %	L.C (ratio)	Y.P %	E.E %	L.C (ratio)
F1	69.72±1.69	77.26±4.06	0.7726±0.031	79.68±22.9	94.6±14.9	0.946±0.012	49.8±5.09	96±11.5	0.96±0.012
F2	49.8±5.36	51.23±6.85	0.5123±0.061	39.8±13.8	83.06±7.95	0.8306±0.09	19.9±6.12	89.3±12.9	0.893±0.058
F3	49.8±8.92	80.5±9.45	0.805±0.093	59.7±6.12	85.04±5.24	0.8504±0.054	39.8±7.49	85.34±7.44	0.8534±0.025
F4	39.8±2.91	51.23±8.61	0.5123±0.0211	29.88±5.14	74.9±6.92	0.749±0.091	10.9±3.94	75.3±6.08	0.753±0.031

Figs. (1-3) showed that the release of drugs from formulae was enhanced significantly at level of $P<0.05$ when compared with drugs only, drugs mixed Tween 80 and drugs mixed with Tween 20 with the same proportions as in the formulae and also commercially available formulations.

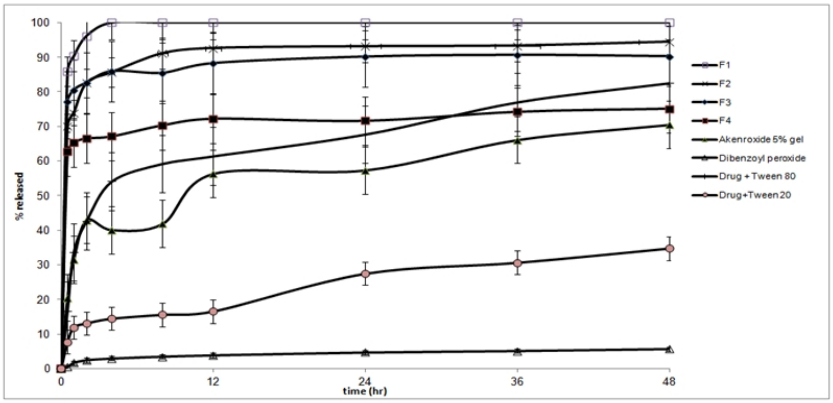

Fig. 1. In-vitro release of DP from SLNs

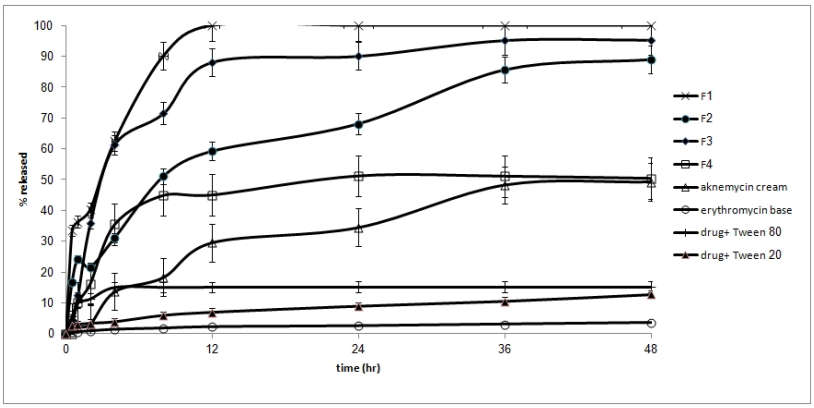

Fig. 2. In-vitro release of ER from SLNs

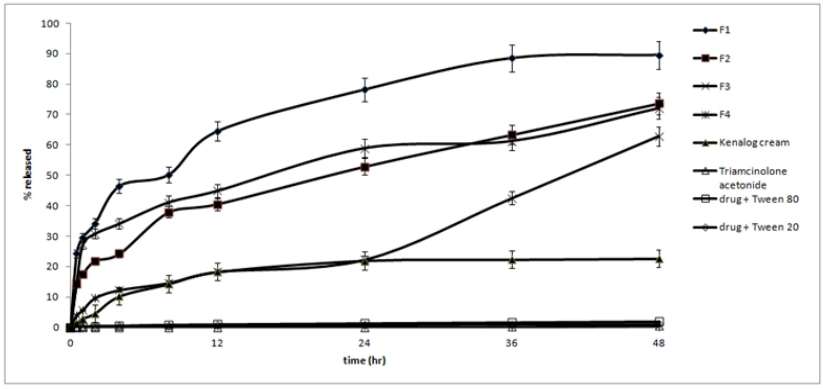

Fig. 3. In-vitro release of TA from SLNs

Upon comparing the release of model drugs from prepared formulae, it was found that formula F1better release efficiency than F3. Tween 80 used for the preparation of F1 gave smaller size than that of Tween 20 used for the preparation of formula F3 with larger micelle size but with lower solubilizing capacity of lipophilic drugs, and hence lower dissolution rate that result in lower release efficiency [21].

The effect of viscosity (50 % Glycerol) on the release of model drugs from prepared formulae were studied as seen in figures (1-3). Glycerol was used as viscosity enhancer during earlier optimization of conditions of SLNs preparation, and resulted in smaller size for the formulae F2 and F4. During release studies, release efficiency of drugs from formulae F1 and F3 were better than that of F2 and F4 that contain 50 % glycerol. Formulae F2 and F4 had a consistency of semisolid form while F1 and F3 still in liquid form which had a good relation to effect of viscosity on release of drugs. According to Bisrat et al [22] who found that viscosity of glycerol affected the rate of dissolution and diffusion of griseofulvin that compatible with our results.

3.4 Scanning Electron Microscopy (SEM)

After loading of different formulations with model drugs, in vitro release studies revealed that formulation F1 showed significant enhancement of release for all model drugs. The formulation showed the best in vitro release discussed earlier were scanned using scanning electron microscope to evaluate surface of formulated solid lipid nanoparticles. Figs. (4-6) show illustrated scans of formulated SLNs loaded with models drugs. From these scans, all SLNs are spherical in shape with smooth surfaces.

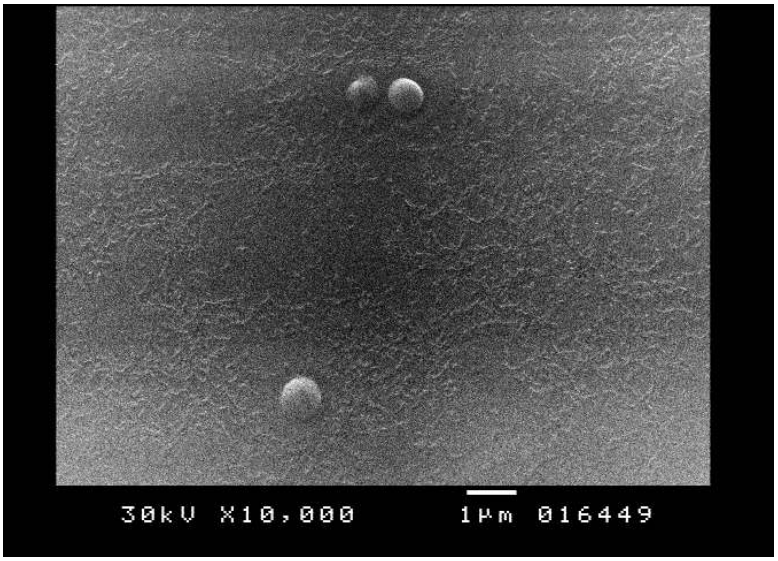

Fig. 4. SE micrograph for DP-SLNs formula F1

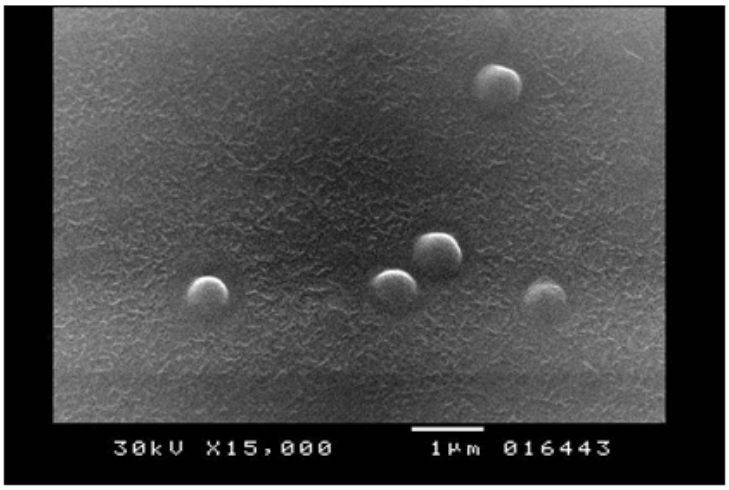

Fig. 5. SE micrograph for ER-SLNs formula F1

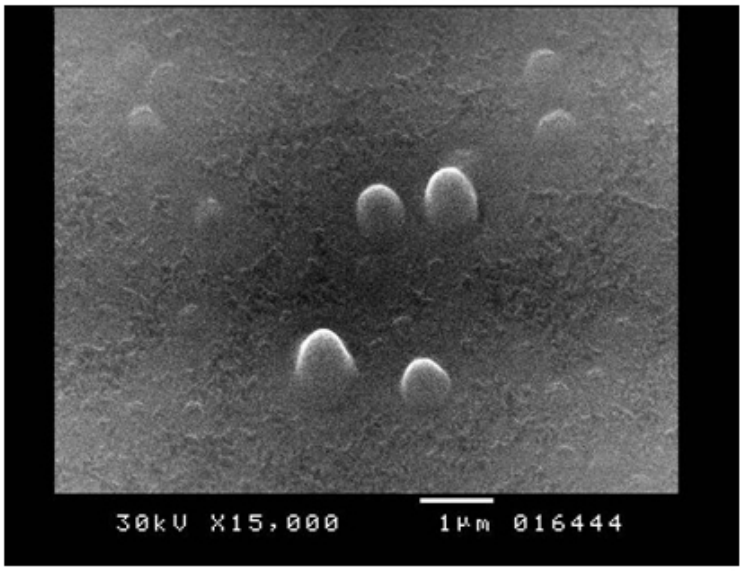

Fig. 6. SE micrograph for TA-SLNs formula F1.

3.5 Transmission Electron Microscope (TEM)

Figures (7-9) show the shape of the nanoparticles entrapping DP, ER and TA. The particles tested demonstrated round and homogeneous shape; the figures also made us sure that the prepared SLNs size was less than 100 nm which agreed with results of Han et al [23] who prepared monostearin nanostructured lipid carriers and studied TEM and found that the particles investigated were round with homogeneous shading and particle size ranging from 50 to 100 nm. The figures illustrated the presence of a layer enclosing the nanoparticles which is characteristic in the case of loaded SLNs. These results in full agreement with Sznitowska et al [24] as they studied the TEM of diazepam loaded SLNs and found a layer

around loaded SLNs that was not apparent in unloaded ones. This is also in agreement with other results of [5,25,26].

It can be fulfilled that the values of SLNs diameters by TEM were clearly smaller than those measured by the particle size analyzer. This may be ascribed to dehydration of nanoparticles during sample preparation for TEM. Also, the particle size analyzer measures the apparent size (hydrodynamic radius) of particles including hydrodynamic layers that form around these nanoparticles leading to overestimation of the nanoparticles size [27,28].

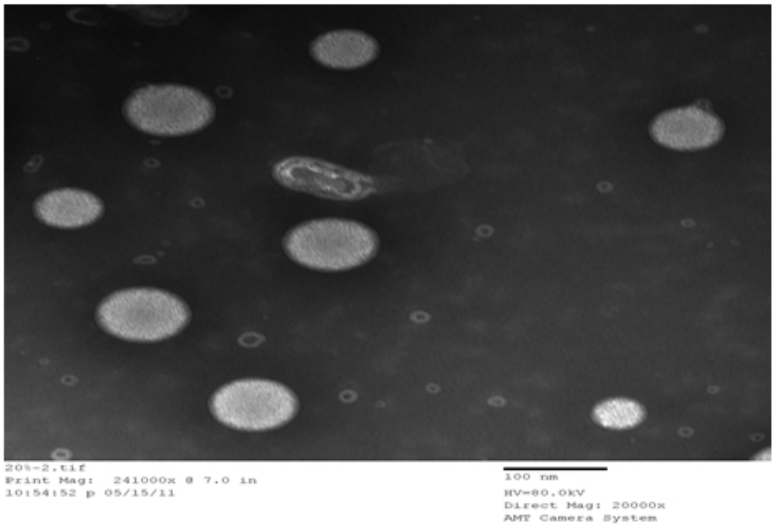

Fig. 7. TE micrograph for DP-SLNs formula F1.

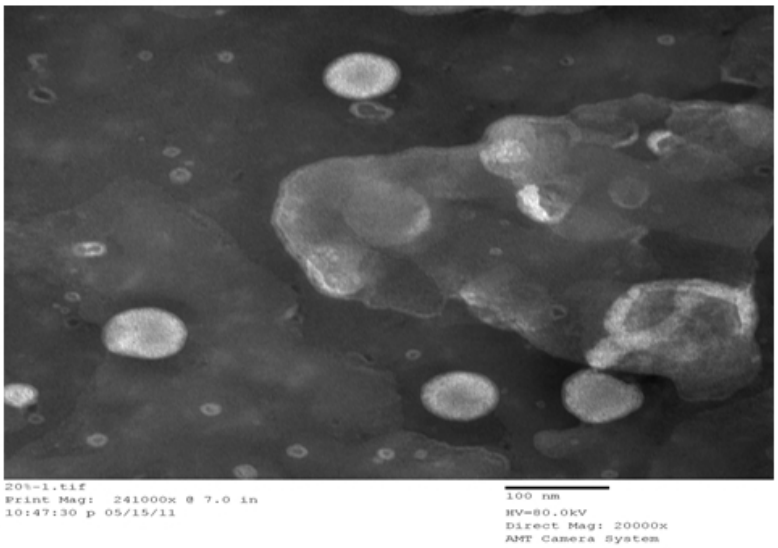

Fig. 8. TE micrograph for ER-SLNs formula F1.

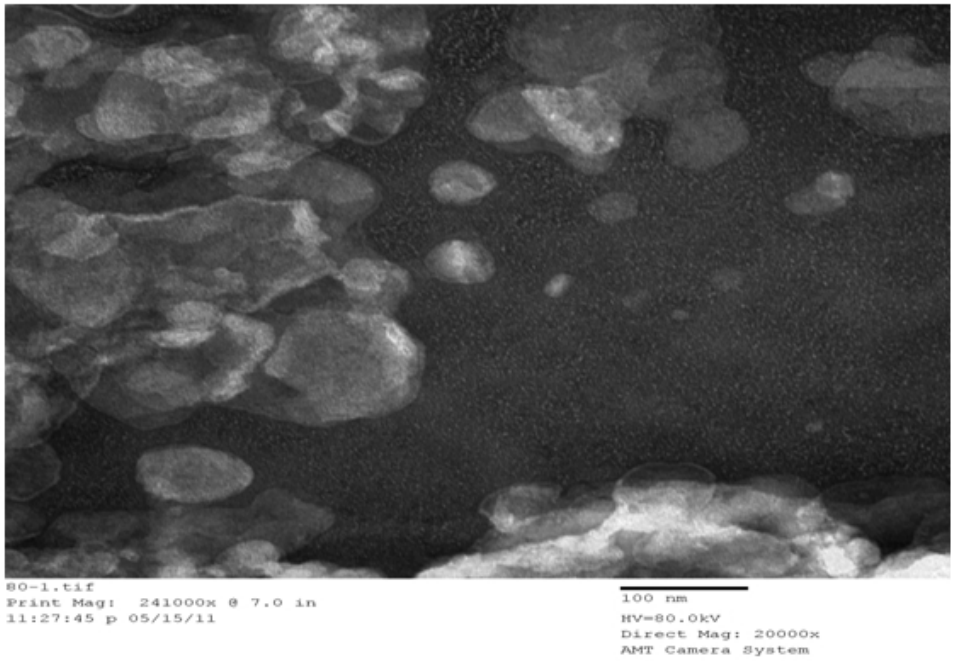

Fig. 9. TE micrograph for TA-SLNs formula F1

3.6 Fourier Transformation Infrared Spectroscopy

Fig (10) showed FTIR spectrum of GMS (lipid core and main component of SLNs). The characteristic bands of it showed C-H stretching and C-H bending at 1200-1000 cm^{-1} and 850- 700 cm^{-1} [29**]**.

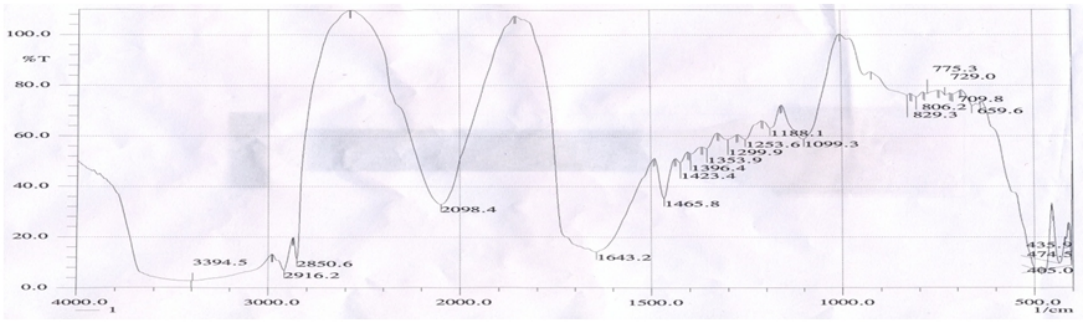

Fig. 10. FTIR spectrum of GMS (main component of SLNs)

Fig (11) showed the FT-IR of DP, physical mixture and DP-SLNs. The characteristic bands of DP include medium weak doublet band of O-O at 1017-880 cm^{-1}, strong band of C-O-O at 1200-1000 cm^{-1}, characteristic aromatic C-H at 3400-3000 $cm^{-1}$and characteristic peak of benzoyl groups at 1727 cm^{-1} .The absence of new bands of DP-SLNs indicated no interaction between drug and lipid matrix, and drug being only dissolved in matrix [30].

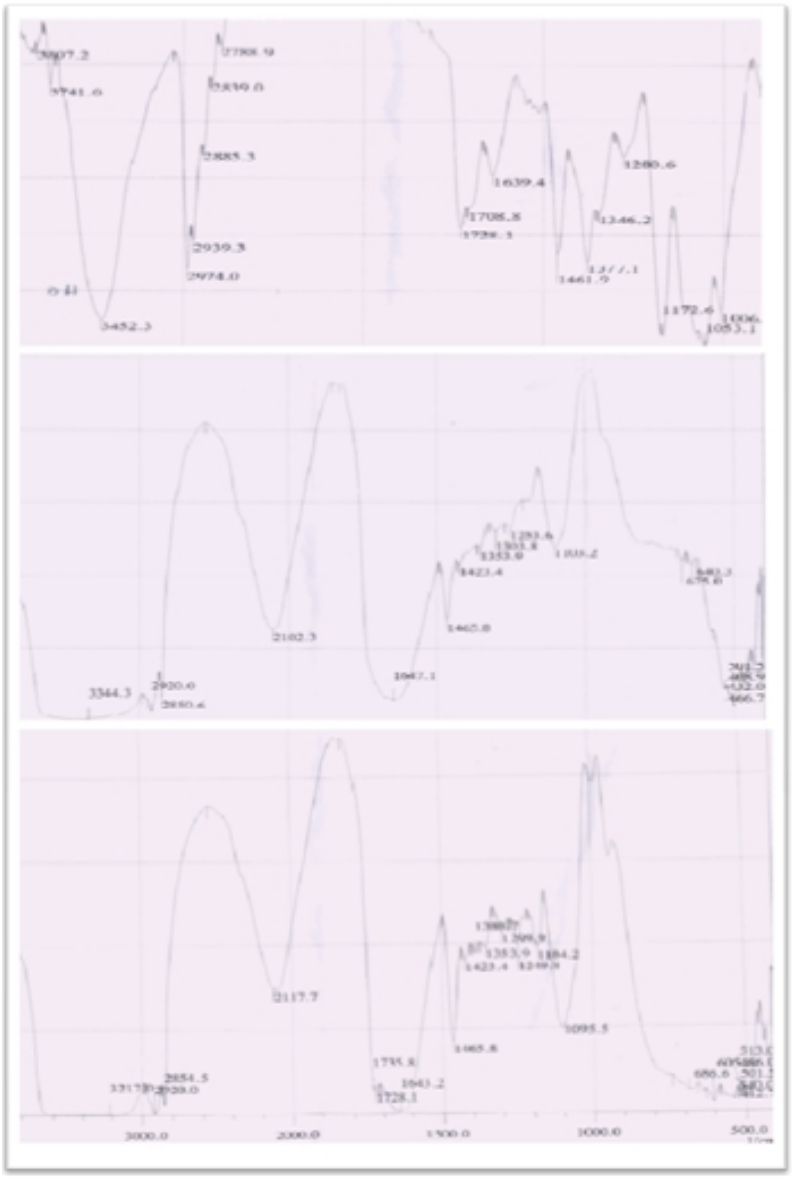

Fig. 11. FTIR spectra of DP, physical mixture and DP- SLNs (formula F1), displaced for better visualization

Figure (12) showed the FT-IR of ER and ER-SLNs which reveal differences in three regions (3300–3700, 2900– 3000, and 1600–1800 cm^{-1}). The small shoulder in the region of 2900–3000 cm^{-1} may be due to the effect of water presented in the molecules on alkane stretching. The difference in intensities of two peaks in the region between 1600 and 1800 cm^{-1} suggests the difference in orientation of carbonyl groups. The absence of new bands of ER-SLNs indicated that there was no chemical reaction between the drug and lipid matrix, being only dissolved in lipid matrix of GMS.These results were in full agreement with that

obtained from Sarisuta et al, [31] who studied the FT-IR of ER loaded on different formulations.

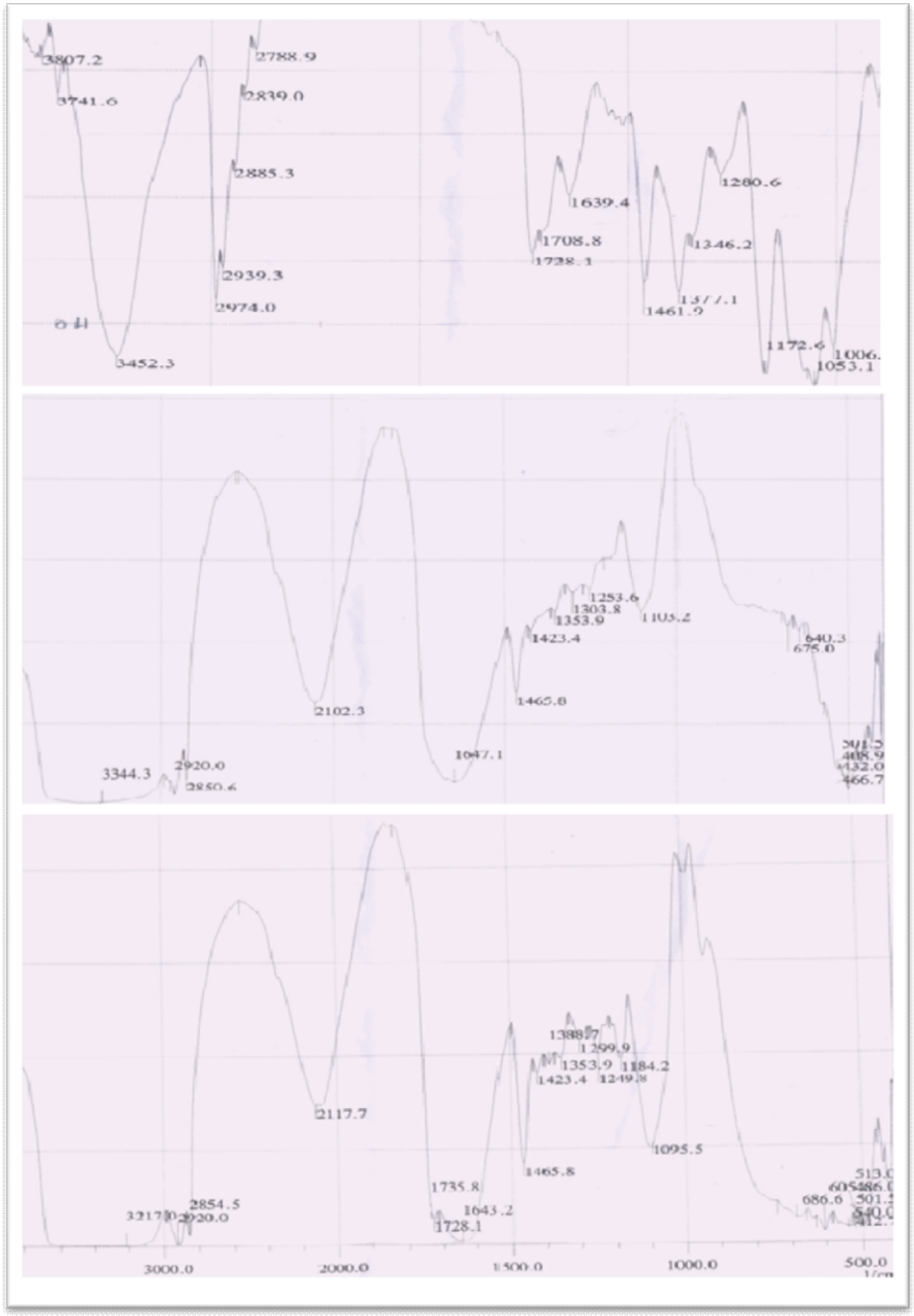

Fig. 12. FTIR spectra of ER, Physical mixture and ER- SLNs (formula F1), displaced for better visualization

In FT-IR spectrum (Fig. 13), the characteristic bands observed from the data of TA included the OH group in the range 3650–3200 cm^{-1}, C–H stretching in the range of 3000 cm^{-1} and 2900 cm^{-1}, C=O in 1775–1650 cm^{-1}, C=C in 1690–1635 cm^{-1}, and C–O–C in 1310–1000 cm^{-1} [29**].** The absence of new bands for TA-SLNs gave indication that there was no chemical interaction between the drug and the lipid, being drug only dissolved in the lipid matrix. Similar results were documented by Da Silva-Junior et al [32) for triamcinolone loaded formulations.

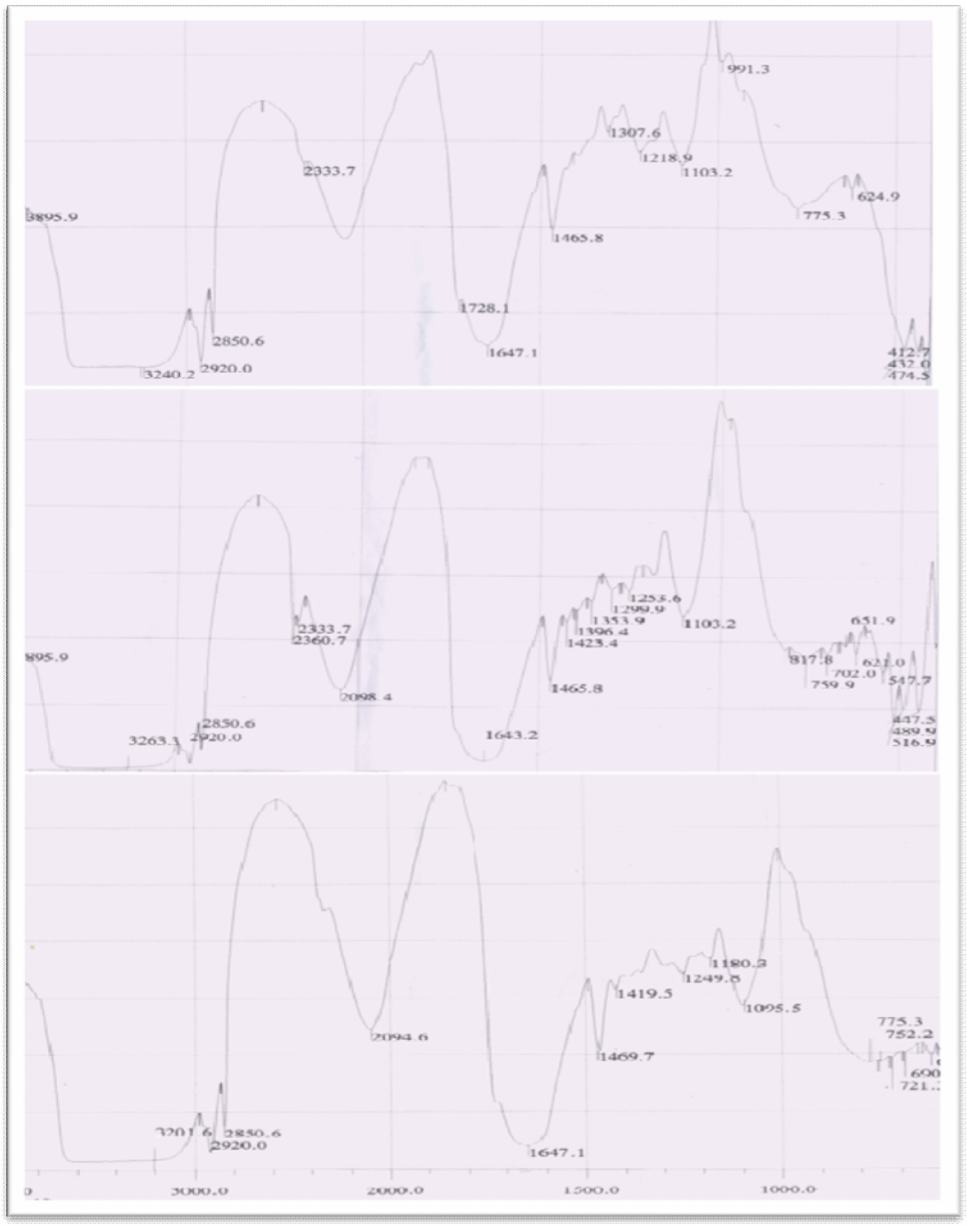

Fig. 13. FTIR spectra of TA, Physical mixture and TA- SLNs (formula F1), displaced for better visualization

3.7 Differential Scanning Calirometry (DSC)

The formula F1 used for loading model drugs due to best release of model drugs was thermally scanned using differential scanning calirometry (DSC). Figure (14) showed DSC thermogram of GMS (main constituent of solid lipid nanoparticles) with sharp endothermic peak around 60 ºC, indicative of melting. These results agreed with that of Freitas et al [33] who studied the DSC analysis of GMS and found that melting endotherm of it was at 60.39 ºC. Figure (15) showed DSC Thermograms of plain SLNs (formula F1) with characteristic peak of GMS reduced to be at 50 ºC approximately. The shift of melting point of GMS may be due to small size (nanometer range) of SLNs compared with lipids in bulk, the dispersed condition of the lipid, and use of surfactants. These results augmented by other literatures [25,26,34,35].

Figure (16) showed DSC thermograms of DP, physical mixture of drug and GMS and DP-SLNs. The thermogram of DP showed very short endothermic peak at 104 ºC followed by sharp exothermic peak around 117 ºC which indicated that the drug was melted followed by degradation. Physical mixture formed of model drug and GMS only. The DSC thermogram of physical mixture showed the characteristic peaks of both GMS at 56 ºC with melting and degradation peaks of DP.

DSC thermogram of DP-SLNs was characterized by initial endothermic peak at 50 ºC approximately which is characteristic for GMS with absence of characteristic exothermic peak of DP which may be indicative of absence drug in crystalline form and solubilization of drug within lipid matrix with enhanced stability.

Fig (17) showed DSC thermograms of ER, physical mixture and ER-SLNs (formula F1). The DSC thermogram of ER showed characteristic ethothermic peaks at 188 ºC, 257 ºC and 294 ºC indicating degradation of drug. DSC thermogram of physical mixture containing ER showed characteristic peak of GMS at 57 ºC with that of ER endothermic peak at 188 ºC, 257 ºC and 294 ºC.

DSC thermogram of ER-SLNs showed the characteristic peak of GMS that shifted to about 50 ºC with absence of endothermic peak of ER indicating solubilization of drug in the lipid matrix of formulated solid lipid nanoparticles.

Fig (18) showed DSC thermograms of TA, physical mixture and TA- SLNs (formula F1).

The DSC thermogram of TA showed characteristic sharp endothermic peak at 288 ºC approximately indicating melting of drug. The DSC analysis of the physical mixture (prepared in the same manner of previous drugs) showed both characteristic peaks of GMS at 60 ºC and of that of TA at 288 ºC. DSC endotherm of TA-SLNs revealed only characteristic peak of GMS with the absence of that of TA indicating solubilization within lipid matrix. These results were in complete fit with that results obtained from Araujo et al. [36].

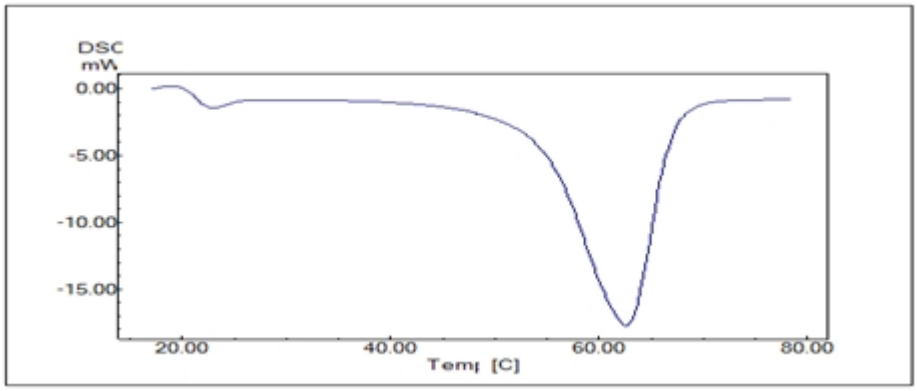

Fig. 14. DSC thermogram of GMS displaced for better visualization

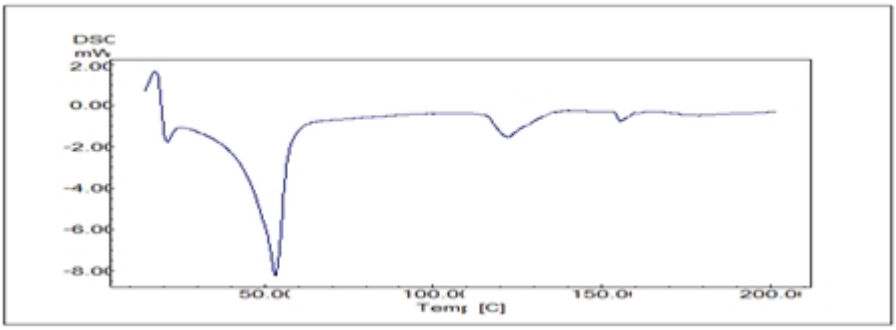

Fig. 15. DSC thermogram of plain SLN (formula F1), displaced for better visualization

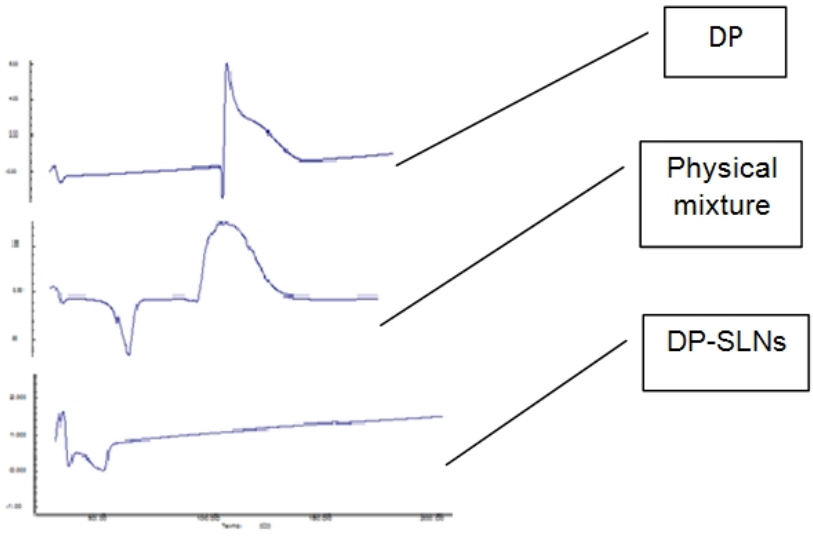

Fig. 16. DSC thermograms of DP, Physical mixture of DP and GMS and DP- SLNs (formula F1), displaced for better visualization

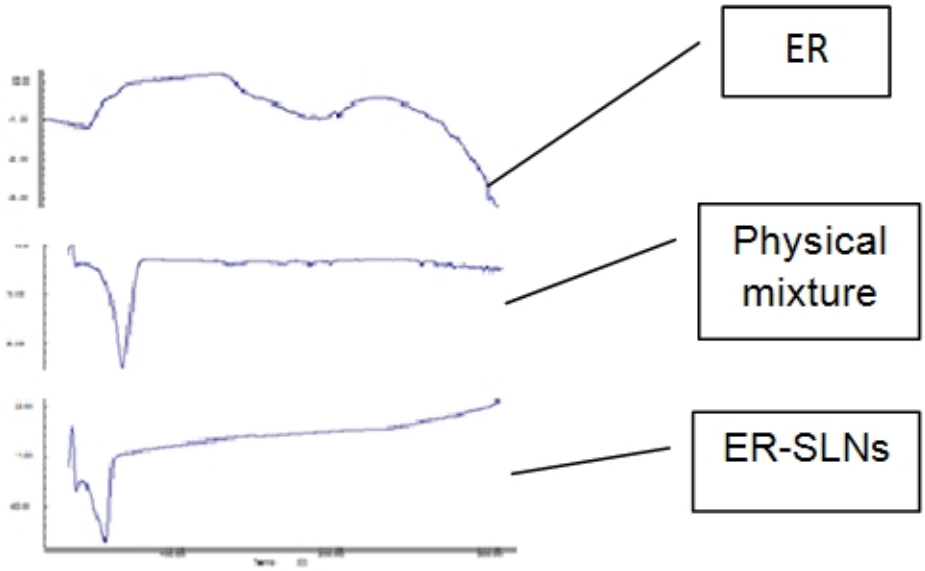

Fig. 17. DSC thermograms of ER, Physical mixture of ER and GMS and ER- SLN (formula F1), displaced for better visualization

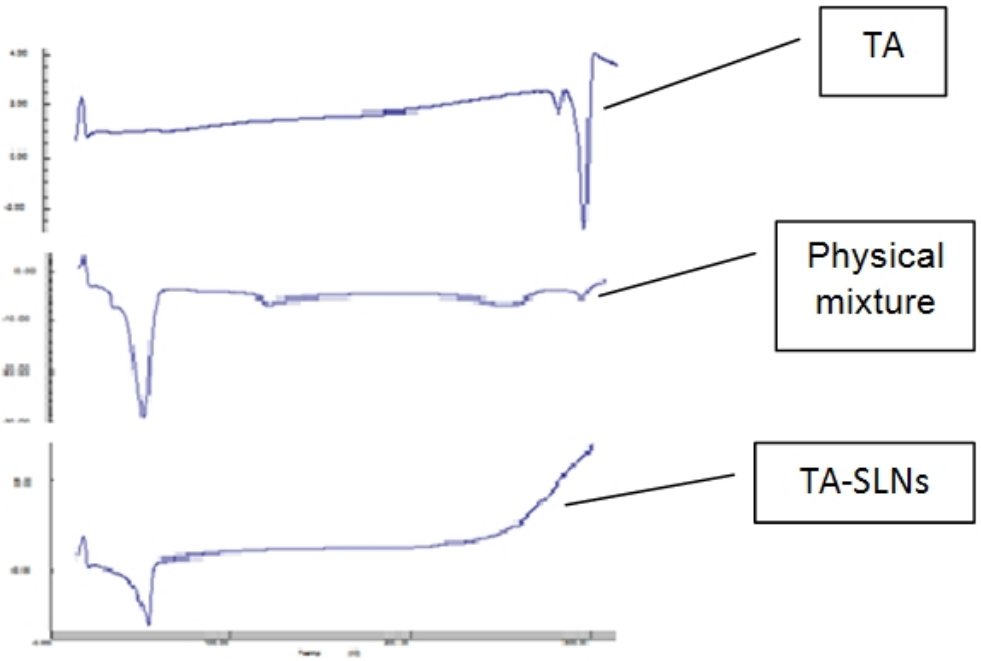

Fig. 18. DSC thermograms of TA, physical mixture of TA and GMS and TA- SLNs (formula F1), displaced for better visualization

4. CONCLUSION

In this study, lipophilic model drugs (Dibenzoyl peroxide, Erythromycin base and Triamcinolone acetonide) were used to study the feasibility of preparation of solid lipid nanoparticles. The drugs were successfully incorporated into SLNs by high-shear hot homogenization technique. The effects of different formulation parameters like viscosity and surfactant type and concentration on encapsulation efficiency, particle size and physicochemical properties of produced SLNs were investigated. Drug release from prepared SLNs formulae was enhanced compared to commercially available formulae as obtained through in vitro release tests. The type of surfactant and also concentration beside glycerol as viscosity enhancer used had a great power on the physicochemical description of SLNs and the in vitro drug release. Formulation F1 containing Tween 80 as a surfactant and the lipid matrix (10% Glyceryl monostearate and 5% Tween 80 with 1 % lecithin as co-surfactant) showed the best results according to the entrapment efficiency and in vitro drug release.

CONSENT

Not applicable.

ETHICAL APPROVAL

Not applicable.

ACKNOWLEDGMENT

The authors are grateful for Suez Canal University for funding the research and MUP Pharmaceutical Company for providing the active ingredient.

COMPETING INTERESTS

Authors have declared that no competing interests exist.

REFERENCES

1. Kumaresh SS, Tejraj MA, Anandrao RK, Walter ER. Biodegradable Polymeric Nanoparticles as Drug Delivery Devices. J. Control. Rel. 2001;70(1-2):1-20.
2. Kiran C, Kuntal G, Mallikarjuna NN, Tejraj MA. Polymeric Hydrogels for Oral Insulin Delivery. J. Control. Rel. 2013;165:129-138.
3. Schwarz C, Mehnert W, Lucks JS, Muller RH. Solid lipid nanoparticles (SLN) for controlled drug delivery. I. Production, characterization and sterilization. J. Cont. Rel. 1994;30:83-96.
4. Raghavendra CM, Ramesh B, Vidhya R, Pradip P, Tejraj MA. Nano/micro Technologies for Delivering Macromolecular Therapeutics using Poly (d,l-lactide-co-glycolide) and its Derivative. J. Control. Rel. 2008;125:193-209.
5. Muller RH, Mader K, Gohla S. Solid lipid nanoparticles (SLN) for controlled drug delivery - a review of the state of the art. Eur. J. Pharm. Biopharm. 2000;50:161-177.

6. Gupta AK, Lynde CW, Kunynetz RAW, Amin S, Choi KL, Goldstein E. A randomized, double- blind, multicenter, parallel group study to compare relative efficacies of the topical Gels 3% Erythromycin/5% Benzoyl Peroxide and 0.025 % tretinoin/ Erythromycin 4% in the Treatment of Moderate Acne Vulgaris of the Face. J.Cuten.Med. Surg. 2003;7(1):31-37.
7. Stecova J, Mehnert W, Blaschke T, Kleuser B, Sivaramakrishnan R, Zouboulis CC, Seltmann H, Korting HC, Kramer KD, Shafer- Korting M. Cyproterone acetate loading to lipid nanoparticles for topical acne treatment: particle characterisation and skin uptake. Pharm.Res. 2007;24(5):991-1000.
8. Schafer- Korting M, Mehnert W, Korting HC. Lipid Nanoparticles for improved topical application of drugs for skin diseases. Adv. Drug. Deliv. Rev. 2007;59:427-443.
9. Yang YY, Wang Y, Powell R, Chan P. Polymeric core-shell Nanoparticles for therapeutics. Clin. Exp. Pharmacol. Physiol. 2006;33:557-562.
10. Mehnert W, Mader K. solid lipid Nanoparticles production, characterization and applications. Adv. Drug. Deliv. Reviews. 2001;47;165-196.
11. British pharmacopoeia. Commission office. British pharmacopoeia. The stationary office, London; 2009.
12. Amin AS, Issa YM. Selective spectrophotometric method for the determination of erythromycin and its esters in pharmaceutical formulations using gentian violet. J. Pharm. Biomed. Anal. 1996;14:1625-1629.
13. Feng W, Jian Y, Yu S, Xing-Guo Z, Fu-De C, Yong-Zhong D, Hong Y, Fu-Qiang H. Studies on PEG-modified SLNs loading vinorelbine bitartrate (I):Preparation and evaluation in vitro. Int. J. Pharm. 2008;359:104-110.
14. Vivek K, Reddy H, Murthy RSR. Investigations of the Effect of the Lipid Matrix on Drug Entrapment, In Vitro Release, and Physical Stability of Olanzapine-Loaded Solid Lipid Nanoparticles. AAPS. Pharm. Sci. Tech. 2007;8(4):article 83.
15. Le Verger ML, Fluckiger L, Kim Y, Hoffman M, Maincent P. Preparation and characterization of nanoparticles containing antihypertensive agent. Eur. J. Pharm. Biopharm. 1998;46:137-143.
16. Almeida AJ, Runge S, Muller RH. peptide –loaded solid lipid Nanoparticles (SLN): influence of production parameters. Int. J. Pharm. 1997;149:255-265.
17. Bhalekar MR, Pokharkar V, Madgulkar A, Patil N. Preparation and Evaluation of Miconazole Nitrate-Loaded Solid Lipid Nanoparticles for Topical Delivery. AAPS PharmSciTech. 2009;10(1):289-296.
18. Kim BD, Na K, Choi HK. Preparation and characterization of solid lipid Nanoparticles (SLN) made of cacao butter and curdlan. Eur. J. Pharm. Sci. 2005;24:199-205.
19. El-Laithy HM, Shoukry O, Mahran LG. Novel sugar esters proniosomes for transdermal delivery of vinpocetine: Preclinical and clinical studies. Europ. J. Pharm. Biopharm. 2011;77(1):43-55.
20. Agnihotri SA, Mallikarjuna NN, Aminabhavi TM. Recent advances on chitosan-based micro- and nanoparticles in drug delivery. J. Control. Rel. 2004;1:5-28.
21. Ghorab MM, Abdel-salam HM, Abdel-Moaty MM. Solid lipid Nanoparticles- effect of lipid matrix and surfactant on their physical characteristics. Bull. Pharm. Sci., Assiut University. 2004;27:155-159.
22. Bisrat M, Anderberg EK, Barnett MI, Nyström C. Physicochemical aspects of drug release. XV. Investigation of diffusional transport in dissolution of suspended, sparingly soluble drugs. Int. J. Pharm. 1992;80(1-3):191-201.
23. Han F, Li S, Yin R, Liu H, Xu L. Effect of surfactants on the formation and characterization of a new type of colloidal drug delivery system: Nanostructured lipid carriers. Coll. Surf. A: Physico. Eng. Aspec. 2008;315:210–216.

24. Sznitowska M, Gajewska M, Janicki S, Radwanska A, Lukowski G. Bioavailability of DZ from aqueous-organic solution, submicron emulsion and solid lipid nanoparticles after rectal administration in rabbits. Eur. J. Pharm. Biopharm. 2001;52:159–163.
25. Muhlen A, Mehnert W. Drug release mechanism of prednisolone loaded solid lipid nanoparticles. Pharmazie. 1998;53:552–555.
26. Muhlen A, Schwarz C, Mehnert W. Solid lipid nanoparticles (SLN) for controlled drug delivery–drug release and release mechanism. Eur. J. Pharm. Biopharm. 1998;452:149–155.
27. Motwani SK, Chopra S, Talegaonkar S, Konchan K, Ahmed FJ, Khar RK. Chitosan – sodium alginate nanoparticles as submicroscopic reservoirs for ocular delivery: formulation, optimization and in vitro chacterization. Eur. J. Pharm. Biopharm. 2008;68:513-525.
28. Prabha FA, Zhou WZ, Panyam J, Labhasetwar V. Size dependency of nanoparticles-mediated gene transfer: studies with fractionated nanoparticles. Int. J. Pharm. 2002;244:105-15.
29. Pretsch E, Bühlmann P, Badertscher M. IR Spectroscopy. Structure Determination of Organic Compounds. Springer, Berlin Heidelberg. 2000;267-320.
30. Pretsch E, Bühlmann P, Badertscher M. IR Spectroscopy. Structure Determination of Organic Compounds. Springer, Berlin Heidelberg. 2009;1–67.
31. Sarisuta N, Kumpugdee M, Muller BW, Puttipipatkhachorn S. Physico-chemical characterization of interactions between erythromycin and various film polymers. Int. J. Pharm. 1999;186:109-118.
32. Da Silva-Junior AA, De Matos JR, Formariz TP, Rossanezi G, Scarpa MV, Do Egito EST, De Oliveira AG. Thermal behavior and stability of biodegradable spray-dried microparticles containing triamcinolone. Int. J. Pharm. 2009;368:45–55.
33. Freitas C, Müller RH. Correlation between long-term stability of solid lipid nanoparticles (SLN$^{(TM)}$) and crystallinity of the lipid phase. Eur. J. Pharm. Biopharm. 1999;47:125–132.
34. Reddy LH, Murthy RS. Etoposide-loaded nanoparticles made from glyceride lipids: formulation, characterization, in vitro drug release, and stability evaluation. AAPS Pharm. Sci. Tech. 2005;6(2):Article 24.
35. Bunjes H, Westesen K, Koch MHJ. Crystallization tendency and polymorphic transitions in triglyceride nanoparticles. Int. J. Pharm. 1996;129:159–173.
36. Araujo J, Mira-Gonzalez E, Egea MA, Garcia ML, Souto EB. Optimization and physicochemical characterization of a triamcinolone acetonide-loaded NLC for ocular antiangiogenic applications. Int. J. Pharm. 2010;393;167-175.

Peer-review history:
The peer review history for this paper can be accessed here:
http://www.sciencedomain.org/review-history.php?iid=211&id=14&aid=1128